ANL/NE-15/40

Rate Theory Modeling and Simulations of Silicide Fuel at LWR Conditions

Nuclear Engineering Division

About Argonne National Laboratory
Argonne is a U.S. Department of Energy laboratory managed by UChicago Argonne, LLC under contract DE-AC02-06CH11357. The Laboratory's main facility is outside Chicago, at 9700 South Cass Avenue, Argonne, Illinois 60439. For information about Argonne and its pioneering science and technology programs, see www.anl.gov.

ANL/NE-15/40

Rate Theory Modeling and Simulations of Silicide Fuel at LWR Conditions

prepared by
Yinbin Miao, Bei Ye, Zhi-Gang Mei, Gerard Hofman, and Abdellatif Yacout
Nuclear Engineering Division, Argonne National Laboratory

prepared for
U.S. Department of Energy
Nuclear Energy Advanced Modeling & Simulation Program

December 10, 2015

ABSTRACT

Uranium silicide (U_3Si_2) fuel has higher thermal conductivity and higher uranium density, making it a promising candidate for the accident-tolerant fuel (ATF) used in light water reactors (LWRs). However, previous studies on the fuel performance of U_3Si_2, including both experimental and computational approaches, have being focusing on the irradiation conditions in research reactors, which usually involve low operation temperatures and high fuel burnups. Thus, it is important to examine the fuel performance of U_3Si_2 at typical LWR conditions so as to evaluate the feasibility of replacing conventional uranium dioxide fuel with this silicide fuel material. As in-reactor irradiation experiments involve significant time and financial cost, it is appropriate to utilize modeling tools to estimate the behavior of U_3Si_2 in LWRs based on all those available research reactor experimental references and state-of-the-art density functional theory (DFT) calculation capabilities at the early development stage. Hence, in this report, a comprehensive investigation of the fission gas swelling behavior of U_3Si_2 at LWR conditions is introduced. The modeling efforts mentioned in this report was based on the rate theory (RT) model of fission gas bubble evolution that has been successfully applied for a variety of fuel materials at devious reactor conditions. Both existing experimental data and DFT-calculated results were used for the optimization of the parameters adopted by the RT model. Meanwhile, the fuel-cladding interaction was captured by the coupling of the RT model with simplified mechanical correlations. Therefore, the swelling behavior of U_3Si_2 fuel and its consequent interaction with cladding in LWRs was predicted by the rate theory modeling, providing valuable information for the development of U_3Si_2 fuel as an accident-tolerant alternative for uranium dioxide.

CONTENTS

FIGURES

TABLES

1. Rate Theory (Model) for Fission Gas Bubble Evolution

Argonne National Laboratory (ANL) has developed two fuel performance codes based on the RT, GRASS-SST and DART, for the simulation of fission gas swelling behavior in nuclear fuels. While GRASS-SST focuses on the evolution of fission gas atom itself and therefore suits the mission of dealing with monolithic form of fuels, DART was designed for handling dispersion form of fuels by involving models capturing the interactions between fuel particles and aluminum matrix. In this report, as we concentrate on using monolithic U_3Si_2 fuels in LWRs, GRASS-SST was employed to perform all the rate theory simulations.

GRASS-SST models the effects of fission-product generation, atomic migration, bubble nucleation and re-solution, bubble migration and coalescence, interlinked porosity, and fission-gas interaction with structural defects [1]. GRASS-SST calculates the fission-gas-bubble-size distribution for bubbles in the lattice, on grain boundaries, on dislocations, and along the grain edges by solving a set of coupled nonlinear differential equations as expressed below:

$$\frac{dC_i^\alpha}{dt} = -a_i^\alpha C_i^\alpha C_i^\alpha - b_i^\alpha C_i^\alpha + e_i^\alpha \qquad (i = \mathbf{1}, \ldots, \mathrm{N};\ \alpha = 1, 2, 3, 4), \tag{1-1}$$

where i is the number of atoms in a bubble; C_i^α is the number density of α-type bubbles in the i^{th}-size class; α = 1, 2, 3, 4 represents the location of the bubbles at the lattice, dislocation, grain-face, and grain-edge, respectively; and the coefficients a_i^α, b_i^α, and e_i^α represent the rates at which α-type bubbles are lost or added to the i^{th}-size class through assorted processes (bubble coalescence, migration process, re-solution/generation, etc.)[1]. Each one of the coefficients a_i^α, b_i^α and e_i^α is dependent on multiple materials properties, such as gas atom diffusivities and gas bubble nucleation and resolution rates. The key materials properties that impact fission gas behavior most, and their values used in this study are listed in Table 1. Detailed description of those materials properties and determination of their values will be presented in Sections II and III.

Those key parameters that determine the gas swelling behavior of nuclear fuels can be further categorized in to two types: lattice related material properties and grain boundary related material properties. The former mainly accounts for the evolution of intragranular fission bubbles, while the latter controls the kinetics of intergranular fission bubbles and gas release. Aside from those material properties, external environment parameters, such as temperature, temperature gradient, fission rate, and hydrostatic pressure, also considerably influence the procedures of fission bubble evolution.
The fission-gas-induced swelling is due to the formation of gas bubbles within fuel during irradiation. In GRASS-SST, the fission-gas-induced swelling $(\frac{\Delta V_{fuel}}{V_{fuel}^0})_g$ is calculated as the summation of gas bubble volumes at all locations and in all size classes, which is

$$(\frac{\Delta V_{fuel}}{V_{fuel}^0})_g = \sum_{i=1}^{N}\sum_{\alpha=1}^{4} C_i^\alpha v_i^\alpha \tag{1-2}$$

where v_i^α is the volume of α-type bubbles in the ith-size class. As the rate theory model only distinguishes the number of fission gas atoms contained by a bubble, the volume of that bubble is determined by a specific equation of state (EOS). For instance, hard sphere EOS is adopted by GRASS-SST to calculate the size of a bubble containing a specific number of gas atoms:

$$(p + 2\gamma / r)(\frac{4}{3}\pi r^3 - nb) = nRT\ , \qquad (1\text{-}3)$$

where, p is the hydrostatic pressure, γ is the surface energy of the fuel material, r is the radius of the bubble assuming a spherical shape, n is the quantity of matter of the gas atoms in the bubble, b is the volume of a single gas atom as in the hard sphere model, R is the gas constant, and T is the thermomechanical temperature.

Table 1: Values of parameters used in the calculations

Category	Parameter	Symbol	Unit
Lattice material properties	Pre-exponential coefficient in gas atom diffusivity	$D_0 (D_g = D_0 \exp(-\frac{Q}{kT}))$	cm^2/s
	Activation energy for gas atom diffusion	Q	cal
	Radiation-enhanced gas atom diffusivity factor	D_g^{RED} $(D_g^{tot} = D_g + D_g^{RED}\dot{f}\ )$	cm^5
	Bubble nucleation factor on grain boundaries	f_n	N/A
	Resolution rate in lattice	$b_0 (b = b_0 \dot{f})$	cm^3
	Fuel surface energy	γ	erg/cm^2
Grain boundary material properties	Multiplication factor to obtain effective irradiation-induced resolution of gas atoms from grain face	$gbr(1)$ $(b_{grainboundary} = gbr(1) \cdot b_0 \cdot \dot{f})$	N/A
	Enhancement factor for gas atom irradiation-enhanced diffusion on grain boundaries	ξ	N/A

Besides the retention of fission gases in fuel, GRASS-SST also accounts for fission gas release from fuel. During fission gas release process, gas atoms diffuse from the grains to grain boundaries and then to the grain edge, where the gas is released through a network of interconnected tunnels of fission-gas and fabrication porosity. The observed formation of grain-surface channels is also modeled, in addition to providing a direct path through which gas residing on the grain surface can reach the grain edges, contributing to intergranular separation and/or cause long-range pore interlinkage. In the fuel temperature regime in this work, there are no bubble movements involved, which become active at very

high temperatures (> 1500°C). For the U_3Si_2 fuel system analyzed in this study, the stresses on cladding are mainly caused by fission-gas-induced swelling not fission gases released from fuel.

The other component of fuel swelling is solid fission product swelling in addition to fission-gas swelling. For solid fission product swelling, no experimental measurements are available. Therefore, estimates are made based on the atomic volume differences between solid fission products and fission-consumed uranium atoms. Solid-fission-product-induced swelling is modeled as linearly proportional to fission density and largely independent on fuel type and temperature **Error! Reference source not found.**. The formulation of $(\frac{\Delta V_{fuel}}{V_{fuel}^0})_{sp}$ can be written as:

$$(\frac{\Delta V_{fuel}}{V_{fuel}^0})_{sp} = \alpha F_d , \qquad (1\text{-}4)$$

where $(\frac{\Delta V_{fuel}}{V_{fuel}^0})_{sp}$ is in %, α is a constant, and F_d is fission density in 10^{21} fissions/cm^3. In this study, α is equal to 1.38, which is suggested by Hofman and Ryu[2] for U_3Si_2 dispersion fuel for test reactors. Based on the bubble size distributions calculated through Eq. (5-1), thermal conductivity of fuel containing fission gas bubbles can be provided at each time step. The fuel thermal conductivity degraded by gas bubble formation is calculated by using the equation as below [3]:

$$k_f^e = k_f(1-(\pi R_g^2(\rho_g)^{2/3})(1-k_g/(2k_f R_g \rho_g^{1/3}))) \qquad (1\text{-}5)$$

where k_f^e is the effective thermal conductivity of fuel that contains fission gas bubbles (W/m-k), k_f is the thermal conductivity of fuel without fission gases (W/m-k), R_g is bubble radius (cm), ρ_g is bubble number density (cm^{-3}), and k_g is the gas thermal conductivity (W/m-k).

2. Parameterization Based on Density Functional Theory (DFT) Calculation

As a state-of-the-art atomistic simulation method, DFT calculation provides solutions of estimating both formation energies and migration energies of specific defect structures. Therefore, it is especially powerful in the investigations on the material properties of systems lacking solid experimental characterizations, such as the material of interest in this report, U_3Si_2. Here, two key material parameters, thermally-activated Xe diffusivity and surface energy of U_3Si_2, were estimated by means of DFT.

2.1 Xe Diffusion in U_3Si_2[4]

According to the most recent communications, Dr. David Anderson's team has obtained a series of diffusion-related parameters of U_3Si_2 system based on precise DFT and extended calculations. In that memorandum, the most valuable and informative results for the RT model are the diffusivity of Xe atom in U_3Si_2 through a variety of mechanisms. These values determine the thermally-activated diffusion of Xe within grains and thus control the evolution of intragranular Xe bubbles. At LWR conditions, due to the increase of temperature, thermally-activated diffusion of Xe is expected to replace radiation-enhanced diffusion (RED) to be the major Xe diffusion mechanism. Hence, a detailed evaluation on how to take a good use of those data is necessary prior to any accurate rate theory calculation.

As multiple migration mechanisms with different Q and D_0 are involved, it is important to look into the dominance of some specific mechanisms at various temperatures. In this report, two representative temperatures, 398 K (typical for low-temperature research reactors applications) and 773 K (typical for LWR applications), were selected. The results are listed in Table 2. As a tetragonal structure material, U_3Si_2 has two different migration directions for Xe atoms, c-axis and a-b plane. Hencem, also illustrated are the logarithm diffusivity vs. reciprocal temperature curves of the two migration mechanisms in both migration directions in Figure 1.

Table 2: Xe diffusivities through different mechanisms at two temperatures

Direction	Mechanism	D_{398K} (m^2/s)	D_{773K} (m^2/s)
c-axis	U-vac 1 to U-vac 1	1.23×10^{-27}	2.58×10^{-17}
	Si-vac to Si-vac	2.32×10^{-54}	4.46×10^{-31}
a-b plane	U-vac 1 to U-vac 1 thru U-vac 2	1.49×10^{-63}	1.54×10^{-35}
	U-vac 2 to U-vac 2 thru Si-vac	8.58×10^{-63}	3.78×10^{-35}
	Si-vac to Si-vac	8.82×10^{-69}	3.46×10^{-38}
	Si-vac to Si-vac thru U-vac	8.62×10^{-69}	3.38×10^{-38}

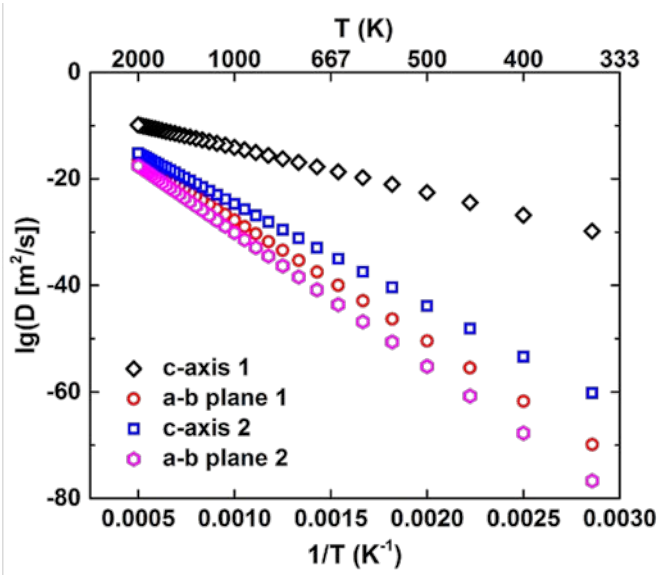

Figure 1: Xe diffusivities through different migration paths

First of all, at both temperatures the mechanism of U vacancy 1 to U vacancy 1 has a diffusivity value that is way much higher than all the other mechanisms. Also, at 398K, even the highest diffusivity is low. Namely, at that temperature, this one-dimensional diffusion mechanism ($<x^2>=2Dt$) only provide a mean square displacement (MSD, or $<x^2>$) of 7.7 $Å^2$ in a year. Thus, at low temperature, the thermally-activated diffusion of Xe is negligible. On the other hand, at 773 K, this mechanism provides a micron level displacement in a year, making significant contribution to Xe diffusion.

Another interesting phenomenon is the anisotropy in diffusivity. In tetragonal crystals such as U_3Si_2, the diffusivities in a-b and c directions usually differ. In U_3Si_2, according to the DFT calculation discussed above, the diffusivity in c direction is greater than that in a-b direction by 36 (298 K) or 18 (773 K) orders of magnitude. Therefore, the Xe diffusion can be regarded as one-dimensional diffusion, namely, $\overline{\overline{D}} = diag\{0,0,D_3\}$. This anisotropy needs to be taken into account for the adoption of this DFT-calculated diffusivity in the rate theory simulation performed by the GRASS-SST code[1].

In GRASS-SST, a grain is assumed to have a spherical shape with radius *R*. Within that grain, the diffusion of Xe atom is governed by a scalar diffusivity, D. Thus, the Xe concentration in that grain, C, follows the following trivial diffusion differential equation:

$$D\frac{1}{r^2}\frac{\partial}{\partial r}\left(r^2\frac{\partial C}{\partial r}\right)+A=\frac{\partial C}{\partial t}. \qquad (2\text{-}1)$$

Meanwhile, if $\overline{\overline{D}} = diag\{0,0,D_3\}$, for the identical grain geometry, we have,

$$D_3\frac{\partial^2 C}{\partial z^2}+A=\frac{\partial C}{\partial t}, \qquad (2\text{-}2)$$

where, A is the constant source term. For simplicity, assume steady state, and C=0 on the grain boundary (surface of the sphere, r=R). In addition, C must be symmetric in spherical geometry (Equation 2-1) or cylindrical geometry (Equation 2-2). Consequently, we have the following expressions for Xe concentrations,

$$C(r) = \frac{A}{6D}(R^2 - r^2), \qquad (2\text{-}3)$$

$$\text{and } C(x,y,z) = \frac{A}{2D_3}(R^2 - x^2 - y^2 - z^2). \qquad (2\text{-}4)$$

Thus, it is appropriate to use $D = D_3/3$ as effective Xe diffusivity in GRASS-SST's RT model. Consequently, in all the simulation described in this report, D_0=7.73×10^{-3} cm^2/s and Q=3.87×10^4 cal.

2.2 Surface Energy of U_3Si_2

As shown in Equation 1-3, surface energy is an important parameter in controlling the size of fission gas bubble. This effect is further illustrated in Figure 2. The figure gives a typical range of the surface energy in solids. For both low and high temperatures and a wide range of bubble scale, the size of a fission gas bubble is highly dependent on the surface energy of the fuel material. Therefore, an accurate assessment of this value plays an indispensable role in the determination of bubble size.

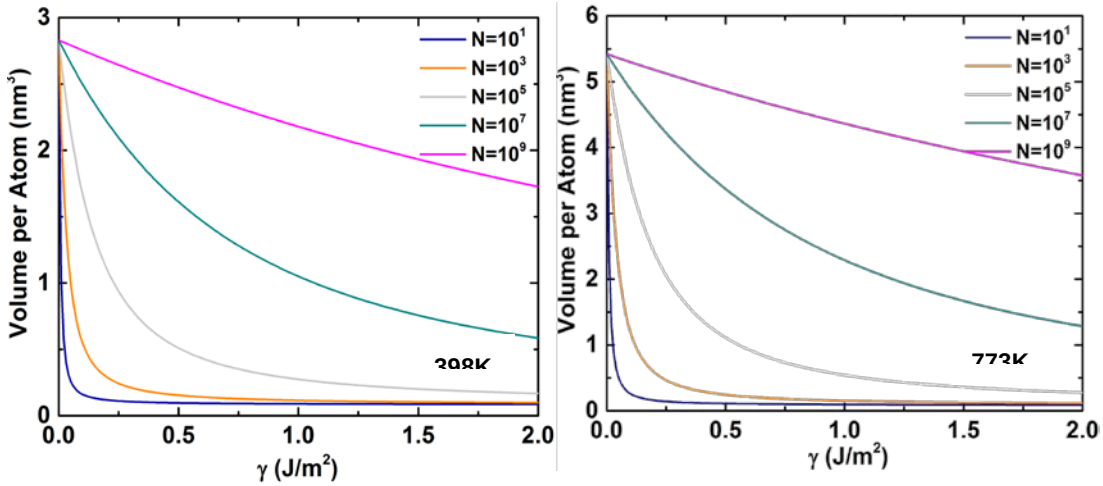

Figure 2.1

Figure 2: Influence of surface energy on the bubble size at low and high temperatures

Again, due to the lack of experimental measurement of the surface energy of U_3Si_2, DFT was utilized to estimate surface energies of surfaces with various Miller indices in U_3Si_2. The same approaches and parameters as used in Section 2.1 were adopted for this task. The surface energy of U_3Si_2 was found to vary from 1.16 to 1.48 J/m^2 depending to different indices. For instance, {100} surface has an energy of 1.48 J/m^2 while {001} surface has an energy of 1.43 J/m^2. For simplicity, 1.32 J/m^2 was selected as the average surface energy and then used in all the RT simulation discussed in this report.

3. Adoption of Low-Temperature Irradiation Experiments Data

3.1 Summary of the Existing Experimental Results for U_3Si_2

As the focus of this project, reasonable prediction of the radiation swelling behavior of U_3Si_2 at LWR conditions is the ultimate task. However, although a great number of irradiation experiments have been conducted for U_3Si_2, none of them were performed at the conditions close to the typical LWR environment. A summary of the previous U_3Si_2 irradiation experiment efforts can be found in Figure 3.

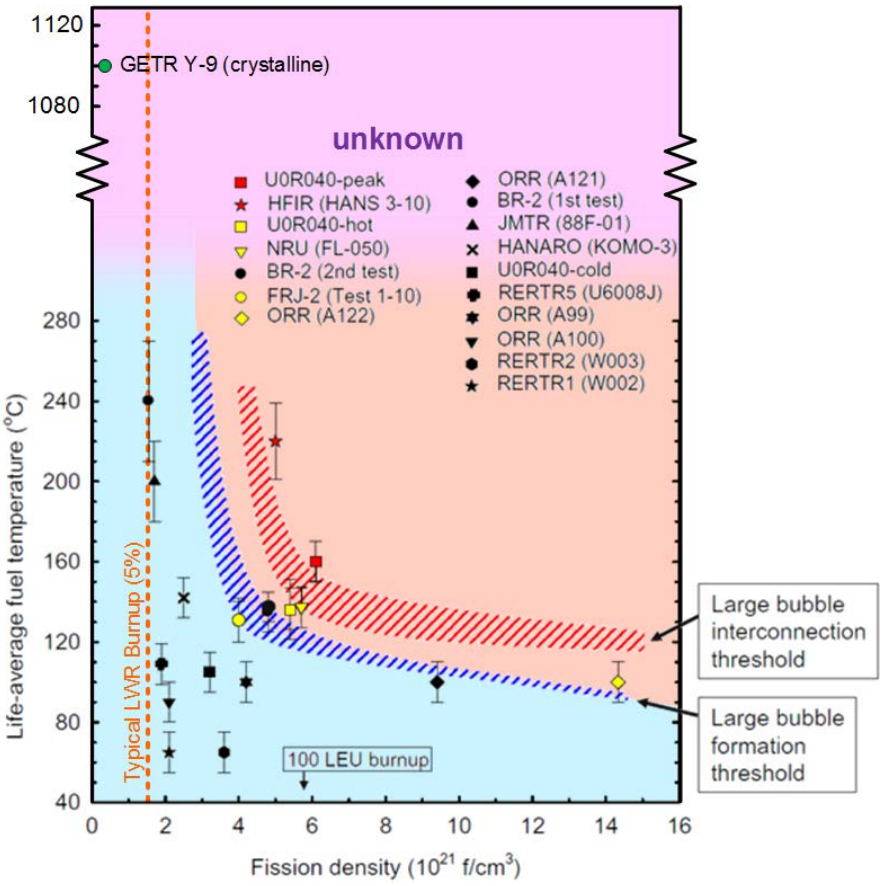

Figure 3: Summary of the conditions adopted by previous U_3Si_2 irradiation experiments [2][5][6]

The majority of the irradiation experiments on U_3Si_2 involve a test reactor environment with a low fuel temperature (which usually does not exceed 300°C) and a high burnup (coupled with higher uranium enrichment)[2][5][7]. At this type of conditions, a threshold was found as shown in Figure 3. Prior to the fission density approaching this threshold, the fuel remains crystalline and experiences limited swelling. No visible gas bubbles can be identified using scanning electron microscopy (SEM) during the post-irradiation examinations (PIEs), implying the gas bubble size is beneath ~10 nm. On the other hand, once the fission density exceeds the threshold, U_3Si_2 fuel turns into amorphous and large gas bubbles form due to the high Xe diffusivity in amorphous phase, causing severe swelling issues and consequent gas release problems. Aside from those low temperature experiments, U_3Si_2 was also once tested in GETR at very high temperature (VHT, >1000°C) in sodium cooling environment[6]. The burnup is though quite low (~2.5×10^{21} fission/cm^3) even compared to typical LWR applications (~1.5×10^{21} fission/cm^3). Large bubbles were observed to accumulate on grain boundaries and then lead

to slight gas release in those fuels. The U_3Si_2 phase remains crystalline, providing a single datum of the irradiation-induced amorphization situation at elevated temperature and low burnup conditions.

At LWR conditions, U_3Si_2 is believed to maintain its crystalline form throughout the entire fuel life-cycle. Thus, only the crystalline stage data of those low temperature research reactor irradiation experiments can be used as references for parameterization of the RT model. On the other hand, the VHT data obtained from the GETR experiment contains abundant information of grain boundary related material properties that determine the fission gas behavior at extreme conditions (e.g. loss-of-coolant accident). Unfortunately, several specific factors limit its application as a valuable reference for the RT model parametrization: 1) the unavailability of the detailed fuel temperature evolution: at this high temperature, the gas behavior is highly sensitive to the temperature, e.g. a difference of 50K in fuel temperature could lead to a difference of 4% (absolute swelling value) in gas swelling. 2) The loss of Si due to the sodium coolant: liquid sodium continues to preferentially dissolve sodium from the fuel, resulting in severe precipitation of U_3Si secondary phase. The U_3Si precipitates affect the precise interpretation of swelling behavior. Therefore, in this study, we focus on the utilization of those LT research reactor data prior to amorphization to retrieve the key parameters used in the RT model.

3.2 Parametrization Based on the Irradiation Experiments

The swelling data from those research reactor irradiation experiments were used to determining some key parameters in the RT model. As those experiments adopted dispersion form fuel elements, the results were transformed to the effective monolithic form values. In particular, the hydrostatic pressure in the fuels of those experiments was selected to be 1233 psi, which is the effective yield stress of aluminum matrix considering radiation creep (this model was used in DART to simulate matrix-fuel interaction). At low temperature, the majority of bubbles stay within the grains. Thus, only those material parameters that are involved in intragranular bubble evolution, such as f_n, b_0, and D_g^{RED}, are expected to be accurately optimized, whereas those grain boundary related parameters, including gbr(1) and ξ, were just given trivial empirical values that work for U-Mo and UO_2 fuel. In this case, f_n, b_0, and D_g^{RED} were determined to be 0.01, 1×10^{-19} cm^3, and 1×10^{-26} cm^2, respectively. Those parameters along with the values determined by DFT method yield the swelling behavior illustrated in Figure 4. A 1.38% per 10^{21} f/cm^3 solid fission product swelling rate was also taken in account in this prediction.

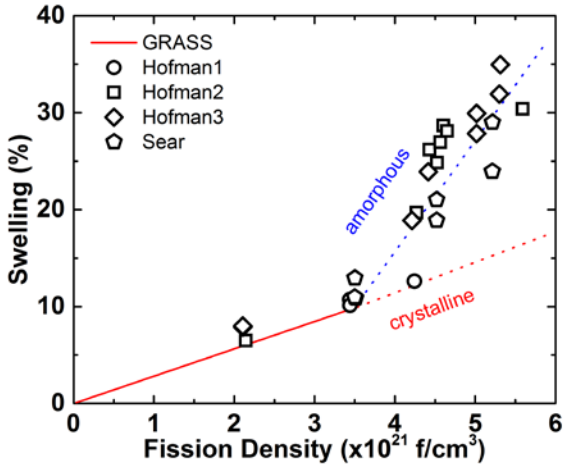

Figure 4: GRASS-SST predicted swelling behavior compared to experimental data [2][7]

As shown in Figure 4, with the optimized parameters, GRASS-SST is capable of replicating the fuel swelling behaviors at low temperatures prior to amorphization. The bubble size distribution was also predicted by GRASS-SST and is illustrated in Figure 5. The overwhelming majority of bubbles are

intragranular and few bubbles are larger than 3 nm in radius. This simulation results are actually perfectly consistent with the PIE observations of those U_3Si_2 fuel irradiated in research reactors. Therefore, the parameterization based on both DFT simulations and LT experiment data was accomplished. Prior to applying those key parameters for the LWR conditions, sensitivity analyses on those parameters need to be performed so as to evaluate the reliability of the results predicted by GRASS-SST.

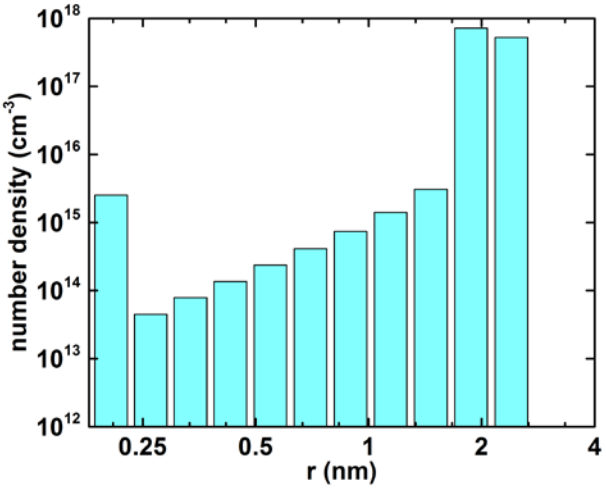

Figure 5: GRASS-SST predicted fission bubble size distribution

4. Sensitivity Analyses on Key Parameters at Low Temperatures

In order to examine how the fluctuations of those key parameters influence the GRASS-SST prediction, the sensitivity of the parameters was also investigated by altering them by approximately an order of magnitude.

As fission gas swelling is dominated by small intragranular bubbles at this temperature, the swelling predicted by GRASS-SST is sensitive to those parameters that control the evolution of the intragranular bubbles. First of all, the nucleation and resolution factors of lattice bubbles, namely, f_n and b_0 (see Figure 6(a)/(b)), are sensitive parameters as they directly affect the kinetics of the intragranular bubble evolution. Meanwhile, as illustrated in Figure 2, surface energy γ also plays an important role in determining the size of fission gas bubbles (see Figure 6(c)). In addition, at low temperature, since thermally-activated diffusion of Xe atoms is hibernated, radiation-enhanced diffusion (D_g^{RED}) drives the evolution of fission gas bubbles (see Figure 6(d)).

On the other hand, those grain boundary related parameters, such as gbr(1) and ξ, play marginal or even negligible parts in the swelling behavior within this low temperature range as few bubbles are located on the grain boundaries, as shown in Figure 7(a)/(b). Therefore, these two parameters were not optimized according to experimental or computational data. Trivial values that work for U-Mo and UO_2 systems were adopted here. As a result, as temperature increases up to ~1000K, the grain boundary bubble behavior predicted by GRASS-SST based on those parameters might not be quantitatively accurate. Thermally-activated diffusion of Xe, described by D_0 and Q, is also irrelevant at low temperature as it is lower than radiation-enhanced diffusivity by orders of magnitude (see Figure 7(d)). Thus, the reliability of those two parameters solely relies on the credibility of the DFT calculation.

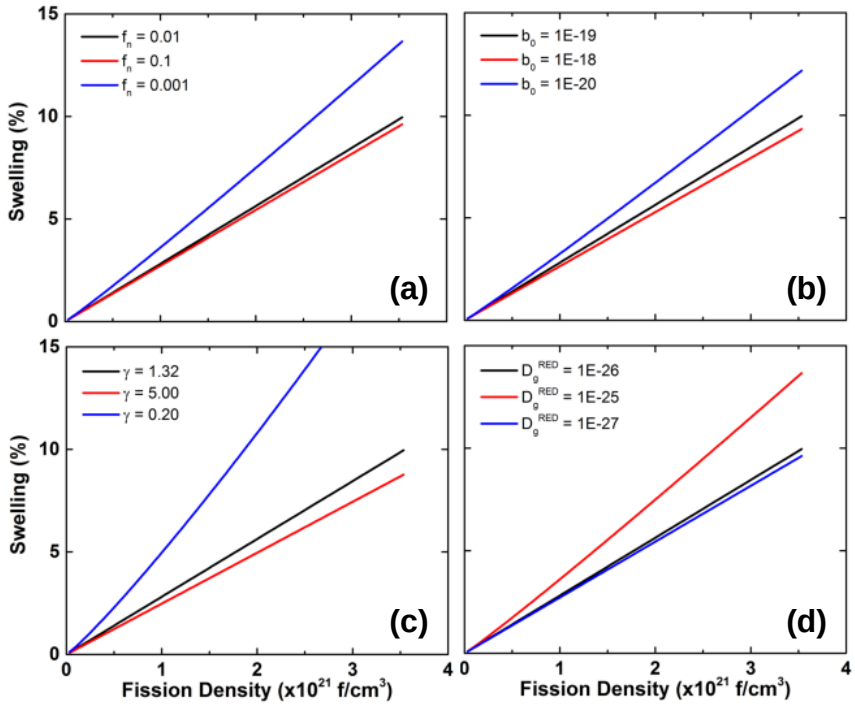

Figure 6: Some sensitive key parameters of the RT model at LT

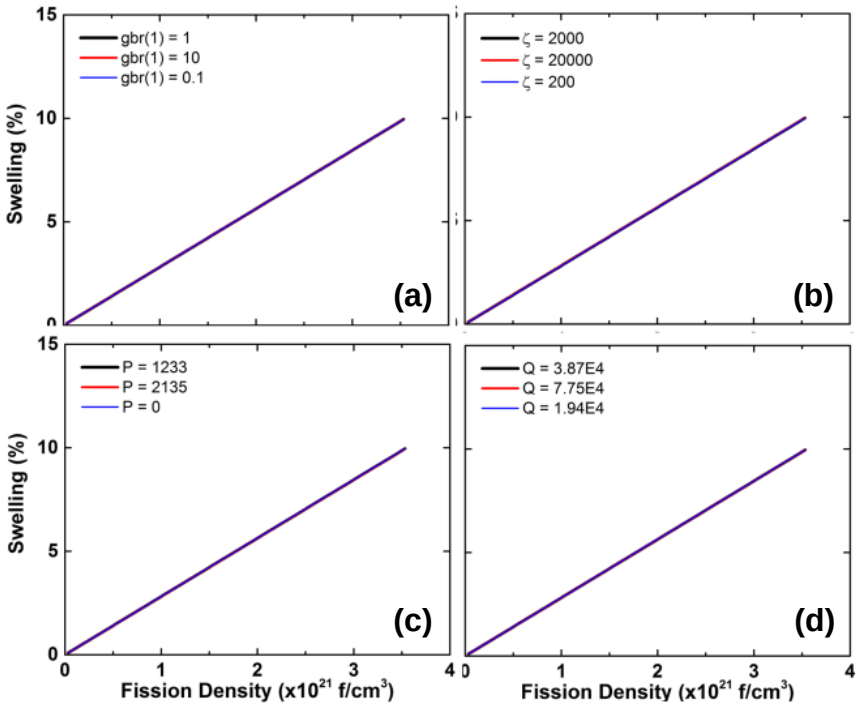

Figure 7: Some insensitive key parameters of the RT model at LT

In addition, as an environment parameter, the external hydrostatic pressure, P, also plays a marginal role at low temperature because the size of small bubbles is mainly controlled by surface energy rather than external pressure.

5. Prediction of Swelling Behavior of U_3Si_2 in LWRs

5.1 Description of the Adopted LWR Conditions

LWRs operate in conditions that vary a lot from those of research reactors, including high fuel temperature and lower burnup. In order to examine the fuel performance of U_3Si_2 in LWRs, the conditions adopted by the GRASS-SST code need to be altered accordingly. As Idaho National Laboratory (INL) did a series of BISON simulations on U_3Si_2 at LWR conditions [8]. For consistency and simplicity, the same conditions were adopted in this study. Some key LWR conditions are listed in Table 3.

Table 3: LWR conditions adopted in this study [8]

Parameter	Unit	Value
Linear average power	W/cm	200
Fast neutron flux	$n/m^2 \cdot s$	9.50×10^{17}
Coolant pressure	MPa	15.5
Coolant temperature	K	530
Fill gas initial pressure	MPa	2.0
Initial fuel density	%	95
Power	MW/tU	35.28
Maximum Burnup	MWd/tU	45000

The rod geometry monolithic U_3Si_2 fuel element was used in the mentioned BISON study, as illustrated in Figure 8. There is no central void reserved for the U_3Si_2 fuel pellets, while the gap width is 80 μm. Ten pellets were contained in a fuel element, which is further clad by Zircaloy-4.

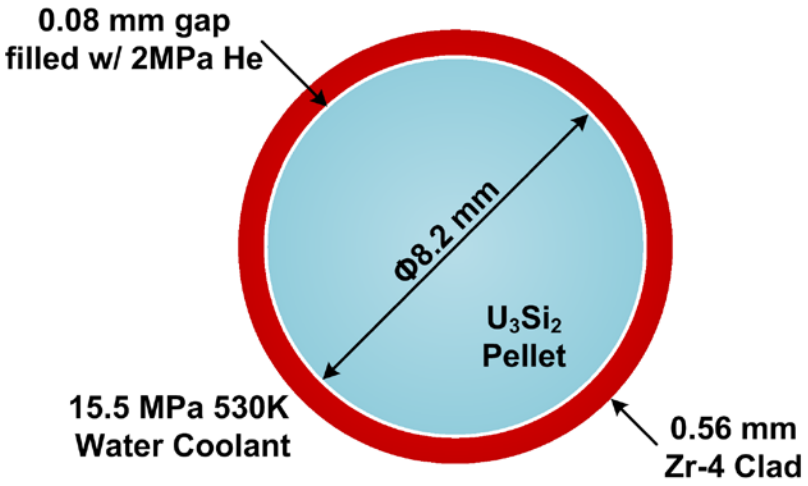

Figure 8: Geometry of the fuel element with design parameters

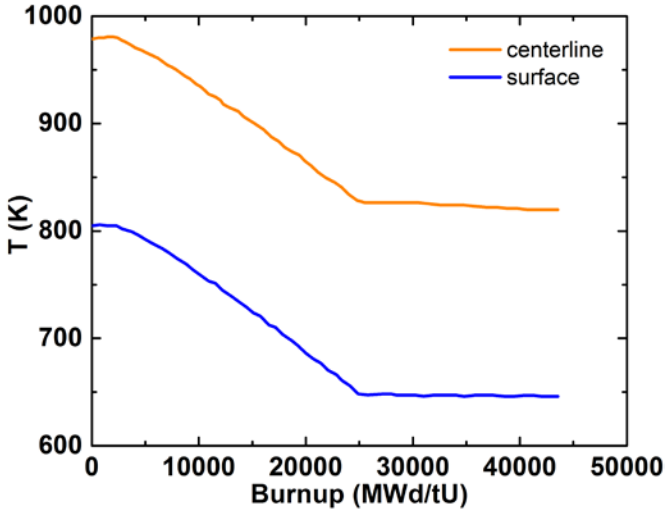

Figure 9: BISON-simulated [8] temperature profile of the U_3Si_2 fuel element throughout the LWR operation

According to the previous BISON simulation, fuel temperature varies with the width of the gap. The temperature-gap width relationship can be approximated to be linear. Also, within the operation temperature range, as the thermal conductivity does not significantly change, a constant temperature difference of ~190K between the centerline and surface of the fuel pellet exist during the entire LWR fuel life-cycle. This 190K difference will be used in this study, while the specific spatial profile of the temperature through the radial direction was believed to follow parabolic shape assuming a uniform fission density.

5.2 Swelling Behavior at Elevated Temperatures

Having the LWR conditions, the swelling behavior can finally be estimated by the RT model. Table 4 summarizes the values of all the key material properties used in the following simulations, which come from DFT calculation, LT experimental data optimization, or trivial values from other classes of fuel materials, as described in detail early in this report.

Table 4: Values of key parameters for simulations at LWR conditions

Parameter	D_0	Q	D_g^{RED}	f_n	b_0	γ	gbr(1)	ξ
Unit	cm^2/s	cal	cm^5	n/a	cm^3	erg/cm^2	n/a	n/a
Value	7.73×10^{-3}	3.87×10^{4}	1.0×10^{26}	0.01	1.0×10^{-19}	1320	1.00	2000

First of all, the temperature effect on the swelling behavior was examined. For simplicity, only one element was used for the entire fuel. Also, the 2MPa initial fill gas pressure was kept constant regardless to the change in temperature. Aside from the fill gas pressure, no other cladding effects were taken into consideration. The swelling results predicted by the GRASS-SST code are shown in Figure 10. Three temperature regimes can be categorized according to those results. As T is lower than approximately 750K (Regime I), the swelling behavior is comparable to that at low-temperature research reactor conditions. The swelling is also due to those small lattice bubbles as in research reactor experiments. When T exceeds ~750K but is still less than ~1000K (Regime II), however, the U_3Si_2 fuel has considerable change in volume. Here the swelling is still dominated by intragranular bubbles so the situation is still controllable. After the temperature is over ~1000K (Regime III), the contribution from grain boundary bubbles starts to be significant. As a result, the swelling first becomes very severe and

then drops due to gas release with the increase of temperature. As mentioned before, the grain boundary related parameters were not optimized. Thus, the quantitative information of Regime III might not be reliable, while the qualitative features of the three regimes is credible. More details about the competition between intragranular and intergranular bubbles can be found in Figure 11.

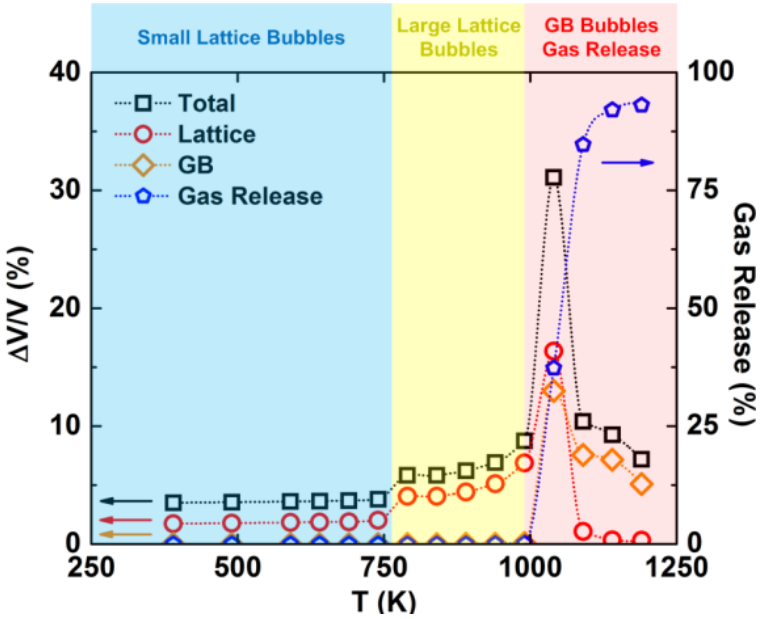

Figure 10: Three swelling regimes predicted by the RT model (T is the average fuel temperature)

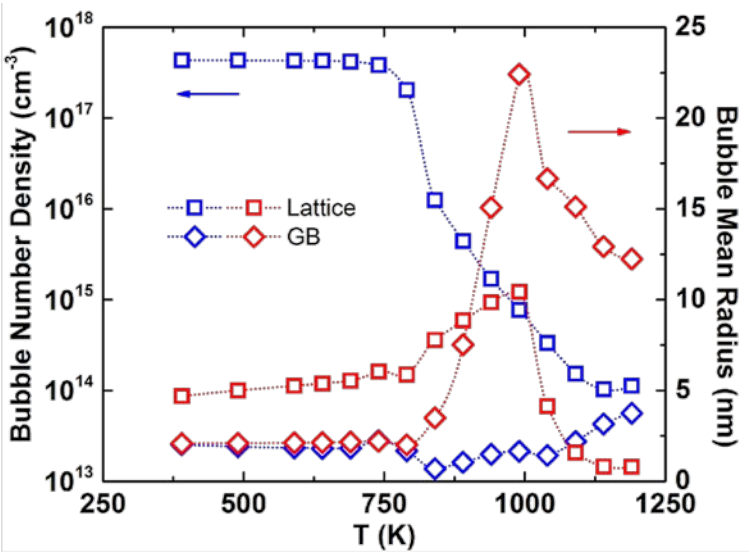

Figure 11: Mean sizes and number densities of bubbles in lattice and on grain boundaries

As the swelling behavior is sometimes sensitive to fuel temperature at LWR temperatures or above, more elements might be necessary so as to capture the bubble evolution precisely. Thus, 1, 5, 10, and 20 elements were tested for different temperature conditions, as shown in Figure 12. If the temperature profile stays in one regime, 1 element is enough to replicate the swelling behavior. However, as the temperature profile crosses two regimes, 10 elements are essential to provide convergent results.

Therefore, 10 elements were used for the fine swelling simulations that will be discussed in next section.

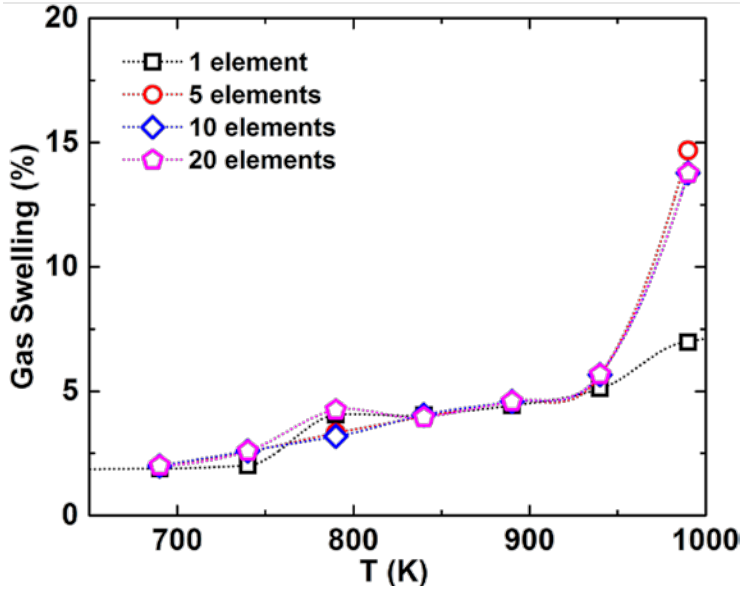

Figure 12: Effect of element numbers at LWR temperature conditions (T is the average fuel temperature)

5.3 Models for Fine Swelling Simulations

Aside from the RT model described above, other simplified models were also involved in the fine swelling simulations at LWR conditions to capture those peripheral parameters. The details of those models are discussed as follows.

First of all, the He fill gas changes its pressure due to the temperature fluctuation and fuel swelling throughout the fuel life-cycle. This change in pressure controls the external hydrostatic pressure of the fuel, especially prior to the gap closure. As the pressure and temperature of the He gas are not extreme, ideal gas equation of state was used to govern this procedure:

$$pV = nRT \quad . \tag{5-1}$$

The helium gas was assumed to maintain 650K constant temperature, while the gas volume is determined by the combined effect of cladding creep-down and fuel swelling.

The fuel densification model was adopted from the previous BISON simulation. In this ESCORE model, the densification strain, ε_D, has the following expression [8]:

$$\varepsilon_D = \Delta\rho_0 \left(e^{\int_0^{Bu} \frac{dt}{Bu_D} \frac{\ln(100)}{C_D(t)}} - 1 \right), \tag{5-2}$$

where $\Delta\rho_0$ is the maximum densification, Bu is the burnup, Bu_D is the burnup point where the maximum densification occurs, C_D is a temperature dependent parameter:

$$C_D = \begin{cases} 7.2 - 0.0086(T - 298) & T \le 750K \\ 1 & T > 750K \end{cases}, \tag{5-3}$$

T is thermodynamic temperature.

The thermal expansion coefficient of the U_3Si_2 fuel was selected as 1.50×10^{-6} K^{-1}[6][8]; the solid fission product swelling rate is 1.38% per 10^{21} f/cm^3, as mentioned before.

The Zorcaloy-4 cladding was assumed to maintain a constant average temperature of 590K. Thus, the Young's modulus is 86.2 GPa, whereas the yield strength is 145 MPa. After yielding, the cladding was assumed to experience perfect plastic deformation without any working hardening. The radiation creep rate, $\dot{\varepsilon}$, was governed by Watkin's empirical model for Zircaloy [9] (only secondary stage was considered):

$$\dot{\varepsilon} = 3.98\times10^{-15}\phi^{0.85}\sinh\left(1.67\times10^{-2}\sigma\right)\exp\left(-14000/RT\right), \quad (5\text{-}4)$$

where ϕ is the fast neutron flus (>1 MeV), σ is the stress, R is the gas constant, and T is the thermodynamic temperature.

The fuel temperature has a difference of 190K between the centerline and the surface and a parabolic shape as discussed before. The surface temperature was assumed to be a linear function of the gap width.

In order to couple the GRASS-SST code with those peripheral models, the code was modified to enable the restart function. The latest version of the GRASS-SST code stores all the variables after each timestep. The code can restart based on those stored data and alteration of those data between timesteps is possible. It is worth mentioning that this code update not only enables the coupling of those peripheral models, but also get the GRASS-SST code prepared for prospective coupling with BISON through MOOSE platform.

5.4 Fine Swelling Simulation for U_3Si_2 at LWR Conditions

The fine swelling simulation was performed based on the models and parameters discussed in the previous sections. The swelling results were compared with the correlation used in the previous BISON simulation, which was based on the low temperature research reactor experiments as shown in Figure 13. It is obvious that the RT model yields a swelling prediction that is higher than the swelling correlation. This is due to the fact that at LWR conditions, the temperature range almost fit Regime II in Figure 10. Hence, unlike the low temperature situation, the intragranular bubbles can be as large as tens of nm. The size distribution of the gas bubbles predicted by the fine swelling simulation is shown in Figure 14. The dominant intragranular fission gas bubbles have a bimodal size distribution as predicted by the RT model. The small-sized group is identical to what was observed at those low temperature research reactor conditions, while the large-sized group (tens of nm) forms due to the increasing diffusivity at elevated temperature. In LWRs, the fuel temperature is not high enough to activate the prominent evolution of bubbles on grain boundaries and the consequent gas release. Here, the GRASS-SST code gives a more credible prediction of the fission gas swelling behavior compared to the simple correlation, showing the advantage of the RT model in assess the radiation swelling phenomenon in U_3Si_2 fuel.

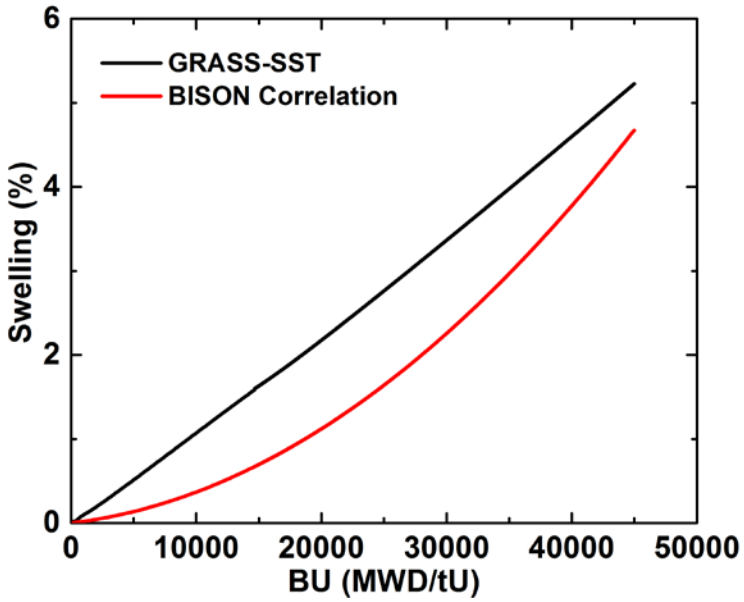

Figure 13: Comparison between the fine swelling simulation and BISON swelling correlation

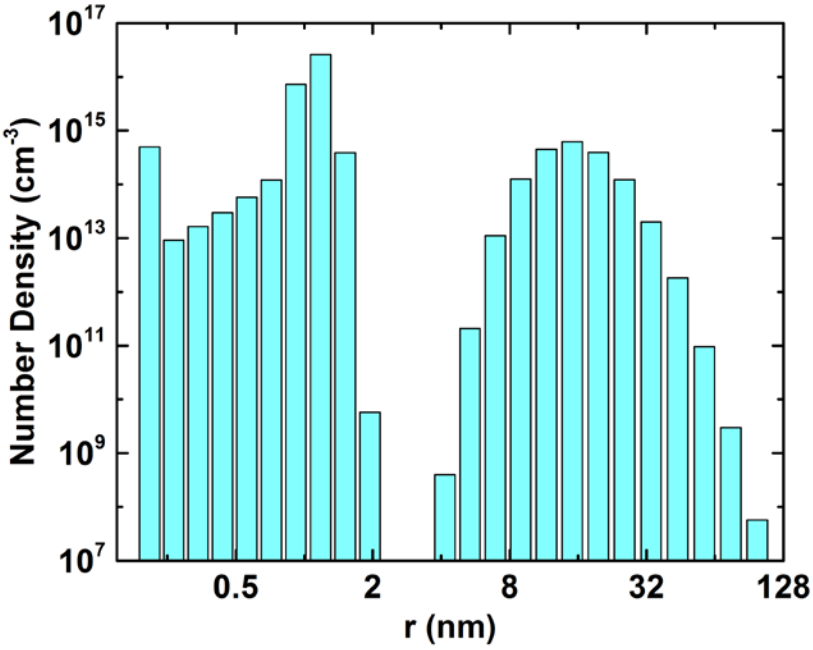

Figure 14: Bimodal size distribution of intragranular gas bubbles

Due to the swelling of the fuel and the creep-down of the cladding, gap closure occurs at approximately 14,000 MWd/tU. Soon after the gap closure, the hoop stress of the Zircaloy-4 cladding flips (see Figure 15), resulting in the corresponding flip of the creep direction (see Figure 16). As the hoop stress increases, the hydrostatic pressure of the fuel also increases (>25 MPa, or 3675 psi). However, this high pressure seems not to significantly affect the swelling behavior shown in Figure 13. This is because those intragranular bubbles of radii around tens of nm are still too small to be compress. Instead, the bubble size is controlled by the surface energy of the fuel.

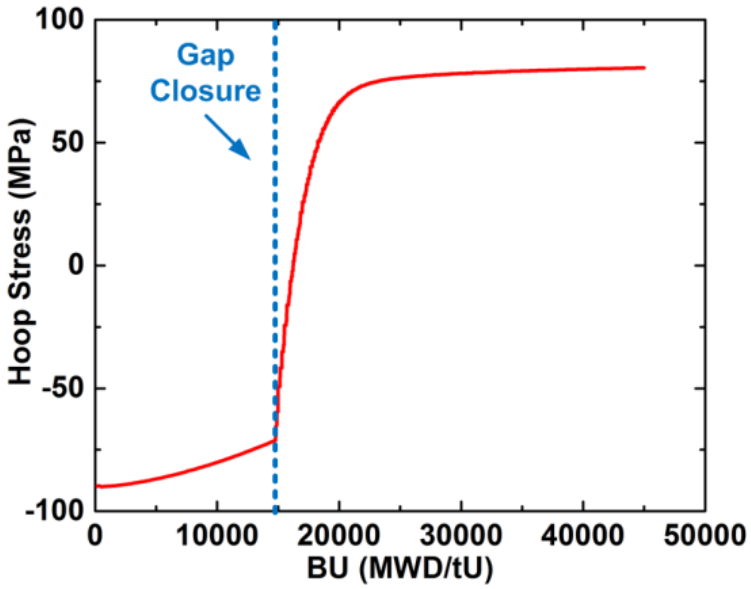

Figure 15: Evolution of the hoop stress of the Zircaloy-4 cladding

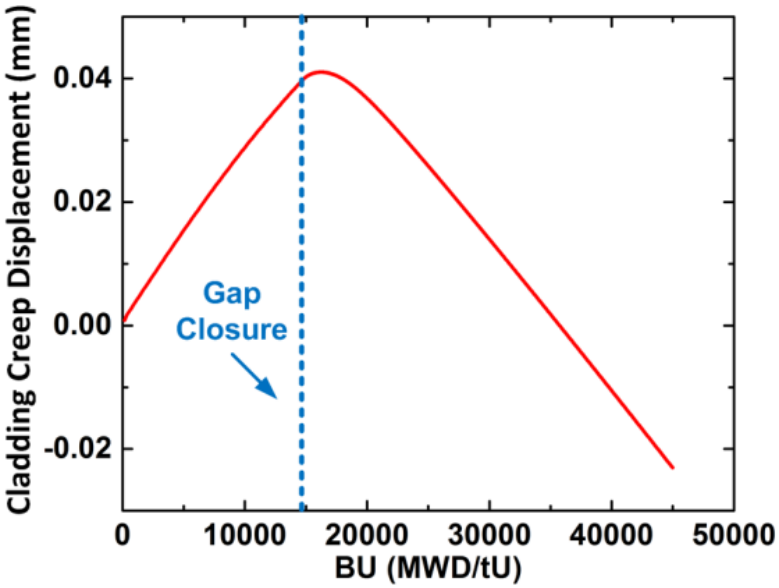

Figure 16: Evolution of the creep displacement of the cladding

The sensitivity analysis on the key parameters is shown in Table 5. As bubble evolution is still limited within the grains rather than on the grain boundaries, the swelling behavior at LWR conditions is still sensitive to Xe diffusivity within grains, f_n, b_0 and γ. Meanwhile, the influence of those grain boundary related parameters, gbr(1) and ξ in particular, is still marginal. At LWR temperature, thermally-activated diffusivity of Xe exceeds the radiation-enhanced diffusivity, being the dominant driving force of bubble evolution. As a result, the swelling results become more sensitive to D_0 and Q compared to D_g^{RED}. It is worth mentioning that the constraint from the Zircaloy-4 cladding limited the swelling behavior in some cases involving prominent increase in swelling rate. For example, decrease in surface energy is supposed to lead to a large increase in swelling. However, pressure from the cladding relieves the severe inflation due to the absence of surface constraint.

Table 5: Sensitivity analysis on key parameters at LWR conditions (Ref: ΔV/V=5.2265%)

Parameter	Unit	Value	ΔV/V (%)
D_0	cm^2/s	7.73×10^{-2}	5.4519
		7.73×10^{-4}	5.1421
Q	cal	7.75×10^{-4}	5.1460
		1.94×10^{-4}	7.4361
D_g^{RED}	cm^5	1.0×10^{-25}	5.2723
		1.0×10^{-27}	5.1569
f_n	n/a	0.1	4.9514
		0.001	5.4851
b_0	cm^3	1.0×10^{-18}	6.1096
		1.0×10^{-20}	4.7743
γ	erg/cm^2	5000	4.0436
		200	8.9119
gbr(1)	n/a	10	5.2387
		0.1	5.2462
ξ	n/a	20000	5.2272
		200	5.2280

5.5 Future Optimization of the RT Model

The parameterization of U_3Si_2 at LWR conditions considered all the existing experimental results and utilized considerable data from DFT calculation. However, in order to further optimize those parameters so as to produce swelling predictions of better confidence, more computational and experimental efforts need to be made to provide more comprehensive references.

For the computational efforts, both thermally-activated diffusivity and radiation-enhanced diffusivity could be optimized based on future DFT calculation and molecular dynamics (MD) simulation. Meanwhile, those grain boundary related parameters may also be examined by MD simulation. On the other hand, before the in-pile-irradiation experiments, which involve significant financial and time costs, can provide realistic fuel swelling data, heavy ion irradiation experiments are capable of providing some valuable information, such as the amorphization threshold position and Xe diffusivity, with a relatively low expenditure.

6. Conclusions

In this study, we optimized the parameter for U_3Si_2 fuel based on coordinated efforts of state-of-the-art DFT calculations and low temperature irradiation experiments. The optimized parameters were utilized for the RT simulation based on the GRASS-SST code to predict the fuel performance of U_3Si_2 at LWR conditions. Multiple peripheral models were taken into consideration to cover majorly the cladding-fuel interaction effects. Both the swelling behavior and the fission gas bubble distribution were predicted by the RT model. At LWR conditions, the RT model predicts that intragranular bubbles dominate the swelling behavior. The reliability of the simulation was examined by performing sensitivity analysis. Further computational and experimental efforts are encouraged to improve the RT model. In addition, the GRASS-SST code was successfully updated with restart capability, which is ready for the prospective coupling with BISON through MOOSE platform.

7. Acknowledgements

This work was supported under US Department of Energy Contract DE-AC02-06CH11357..

8. References

[1]J. Rest, “GRASS-SST: a comprehensive mechanistic model for the prediction of fission-gas behavior in UO_2-base fuels during steady-state and transient conditions,” NUREG/CR-0202, Argonne National Laboratory, Report ANL-78-53 (1978).

[2] G.L. Hofman and Woo-Seog Ryu, “Detailed analysis of uranium silicide dispersion fuel swelling”, Proceedings of the RERTR International Meeting, (1989)

[3] J. Rest, “The DART Dispersion Analysis Research Tool: A Mechanistic Model for Predicting Fission-Product-Induced Swelling of Aluminum Dispersion Fuels,” ANL-95/36, Argonne National Laboratory (1995).

[4] D. Andersson, NEAMS-HIPS ATF Program Memorandum, (2015)

[5] Y.S. Kim, G.L. Hofman, J. Rest, and A.B. Robinson, J. Nucl. Mater. 389 (2009) 443-449

[6] H. Shimizu, Atomics International Report NAA-SR-10621, (1965)

[7] D.F. Sears, “Development and irradiation testing of Al-U_3Si_2 fuel at Chalk River Laboratories”, Proceedings of the RERTR International Meeting, (1991)

[8] K.E. Metzger, T.W. Knight, and R.L. Williamson, INL Report CON-13-30445, (2014)

[9] B. Watkins, D.S. Wood, “The significance of irradiation-induced creep on reactor performance of a Zircaloy-2 pressure tube,” ASTM Selected Technical Papers, 458, 226-280 (1969)

Nuclear Engineering Division
Argonne National Laboratory
9700 South Cass Avenue, Bldg. 208
Argonne, IL 60439

www.anl.gov